

Supporting Information for:

**Morphological transitions in chemically fueled self-assembly**

**Authors:** Kun Dai,<sup>a</sup> Marta Tena-Solsona,<sup>a</sup> Jennifer Rodon Fores,<sup>a</sup> Alexander M. Bergmann,<sup>a</sup> and Job Boekhoven<sup>\*a,b</sup>

**Affiliations:**

<sup>a</sup> Department of Chemistry, Technical University of Munich, Lichtenbergstrasse 4, 85748 Garching, Germany.

<sup>b</sup> Institute for Advanced Study, Technical University of Munich, Lichtenbergstrasse 2a, 85748 Garching, Germany.

## Materials and methods

**Materials.** All reagents were purchased from Sigma-Aldrich and Alfa-Aesar and used without further purification unless otherwise indicated. The peptides used in this study were synthesized using solid-phase peptide synthesis.

### Peptide synthesis and its purification.

#### Ac-FIVD, Ac-FILD-OH, Ac-FVVVD-OH, Ac-FIVVD-OH

The peptide synthesis was performed on a CEM Liberty microwave-assisted peptide synthesizer. The first amino acid coupling to the resin was accomplished by using the symmetrical anhydride method. Briefly, a 0.2 M solution of the symmetrical anhydride was prepared by allowing the Fmoc-protected aspartic acid (FmocD(OtBu)OH, 12 mmol) and N,N'-diisopropylcarbodiimide (DIC, 6 mmol) to react in 30 mL N,N-dimethylformamide (DMF) for 60 min. The solution was placed in a freezer at -20 °C for 30 min, and the solid urea formed was filtered out before the next step. Loading of the resin was performed using the automated peptide synthesizer. The symmetrical anhydride solution (0.2 M, 12 mL) and 4-(dimethylamino)pyridine (DMAP) solution in DMF (20 mM, 2.5 mL) were added to the pre-swollen Wang resin (0.5 mmol, 1.1 mmol/g) and heated in the microwave (30 min, 75 °C). The coupling was repeated twice. The resin was then washed with DMF (2x10 mL). Following couplings were achieved using 4 equivalents (eq.) of Fmoc-protected amino acid in DMF, 4 eq. of DIC and 4 eq. of ethyl (hydroxyimino)cyanoacetate (Oxyma). The resin solution was then heated in the microwave (1x2 min, 90 °C). Fmoc removal was accomplished using a solution of 20% piperidine in DMF (1x2 min, 90 °C). The resin was washed with DMF (3x7 mL) between different steps. This procedure was repeated until the last chemical CH<sub>3</sub>COOH was coupled. The resulting peptide was cleaved from the resin using a mixture of 95% trifluoroacetic acid (TFA), 2.5% water, and 2.5% triisopropylsilane (TIPS). The solvent was removed by co-distillation with DCM by rotary evaporation and dried under reduced pressure. The residue was extracted with diethyl ether one time and the organic phase was washed two times with water. The combined aqueous phase was purified using reversed-phase high-performance liquid chromatography (HPLC, Thermofisher Dionex Ultimate 3000, Hypersil Gold 250x4.8 mm) in a linear gradient of acetonitrile (ACN, 2% to 98%) and water with 0.1% TFA. The purified peptide was lyophilized and stored at -20 °C until further use. (See Supporting Table 1 for a summary of the analysis of the peptides).

### Methods.

**Sample preparation.** Stock solutions of the precursors were prepared by dissolving the peptides in 200 mM MES buffer, after which the pH was adjusted to pH 6.0 with NaOH solution. Stock solutions of EDC were prepared by dissolving the EDC powder in MQ water.

These stock solutions were used freshly. The reaction cycles were initiated by the addition of the EDC to the precursor solution. We carried out all experiments at 21.5 ( $\pm 0.5$ ) °C.

### **Analysis of the reaction kinetics by HPLC.**

Analytical reversed-phase HPLC experiments were performed on a ThermoFisher Dionex Ultimate 3000 liquid chromatography setup (Dionex Ultimate pump, Dionex Ultimate Autosampler, Dionex Ultimate 3000 RS Variable Wavelength Detector, Hypersil Gold 250 x 4.6 mm, C18 column (5  $\mu$ m pore size)). The standard detection wavelengths were set to 220 and 254 nm. For quantification of the anhydride concentrations during the reaction cycle, a quenching method with benzylamine previously reported was used<sup>1</sup>. Specifically, after the reaction cycle was started by the addition of EDC fuel, 10  $\mu$ L of the corresponding sample were pipetted on 30  $\mu$ L of a 500 mM benzylamine solution in Acetonitrile (ACN) in a 200  $\mu$ L HPLC vial inlet and mixed by pipetting and vortexing. The turbidity, vanished completely during the quenching and mixing process. Additionally, the pH of the quenched mixtures increased instantly to 9.3 which also inhibits further hydrolysis of the remaining EDC during the analysis and stops the reaction cycle. We used a linear gradient from 98:2 to 2:98 in 10 minutes followed by 2 minutes at 2:98 for the separation. The column was equilibrated for 2 minutes after each gradient. Retention times are given in Supporting Table S1. The peptide anhydride concentrations were quantified from the corresponding peptide-benzylamide peaks (Fig. S1 - Fig. S4). The calibration value for the **P1** peptide-benzylamide is 0.76, **P2** peptide-benzylamide is 0.75, **P3** peptide-benzylamide is 0.81, and **P4** peptide-benzylamide is 0.81.

**Kinetic model.** A kinetic model was used to predict the evolution of the anhydride concentration over time. The model is described in detail in the Supporting Note 1. The rate constants we used in this work are given in Table S2.

**UV/Vis Spectroscopy.** Turbidity measurements were carried out at 21.5 °C on a Microplate Spectrophotometer (Thermo Scientific Multiskan GO, Thermo Scientific SkanIt Software 4.0). Measurements were performed in a non-tissue culture treated 96-well plate (Falcon, flat bottom). Every minute, the absorbance of the 200  $\mu$ L samples was measured at 600 nm. All experiments were performed in triplicate (n=3).

**ESI-MS.** ESI-MS experiments were conducted on an LCQ Fleet Ion Trap Mass Spectrometer (Thermo Scientific). Interpretation of all recorded MS data was performed using the Thermo Xcalibur Qual Browser 2.2 SP1.48 software.

**Confocal Fluorescence Microscopy.** Confocal Fluorescence Microscopy. Confocal fluorescence microscopy was performed on a Leica TCS SP8 confocal microscope using a 63x water immersion objective. Samples were prepared as described above and transferred

into micro-well plates (ibidi,  $\mu$ -Slide Angiogenesis Glass Bottom). 2.5  $\mu$ M *Nile red* was added as fluorescent dye. Samples were excited with 552 nm and imaged at 565-635 nm.

### Determination of the solubility of the anhydride.

Samples of **P1** (10 mM), **P2** (10 mM) **P3** (10 mM) and **P4** (10 mM) were fuelled with different amounts of EDC and the mixtures were analysed over time by HPLC and UV-Vis (absorbance at 600 nm). When the amount of EDC was not enough to reach the value of the anhydride's solubility, no turbidity was observed. After a certain EDC concentration, turbidity appeared. The maximum concentration of anhydride obtained with this EDC concentration was compared with the maximum concentration of anhydride of the closest EDC concentration trace that did not show any turbidity over time. The solubility value for the anhydride was then established between these two maxima with the corresponding error.

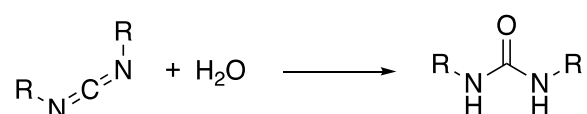
### Supporting note 1: Description of the kinetic model

A kinetic model was written in Matlab that describes each reaction involved in the chemical reaction network except. The concentrations of each reactant were calculated for every second in the cycle. The model was used to fit the obtained HPLC data that described the evolution of the concentration of anhydride, EDC and acid over time. In all experiments, the concentration of the precursor was 10 mM.

The model described five chemical reactions:

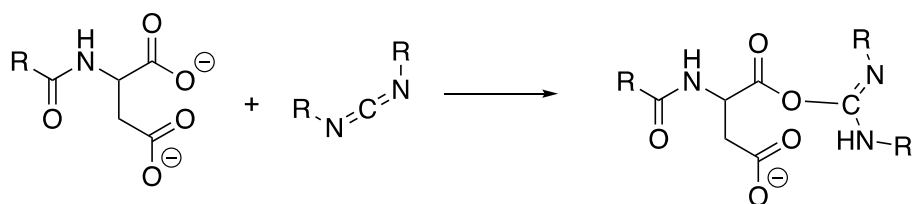
0) Direct hydrolysis of carbodiimide with a first order rate constant of  $1.3 \times 10^{-5} \text{ sec}^{-1}$  as determined in previous work.

Reaction 0 ( $k_0$ )



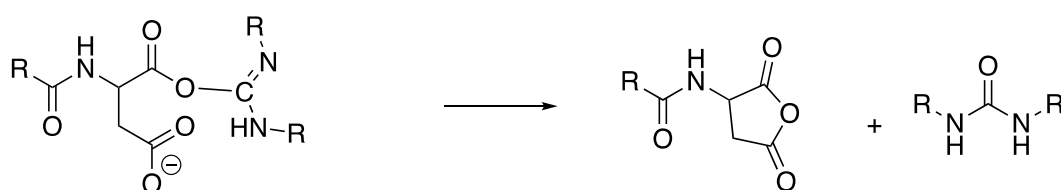
1) The formation of O-acylurea by reaction with EDC ( $k_1$ ). This second order rate constant was dependent on the nature of the precursor. The rate constant was determined for each precursor by HPLC, by monitoring the EDC consumption.

Reaction 1 ( $k_1$ )



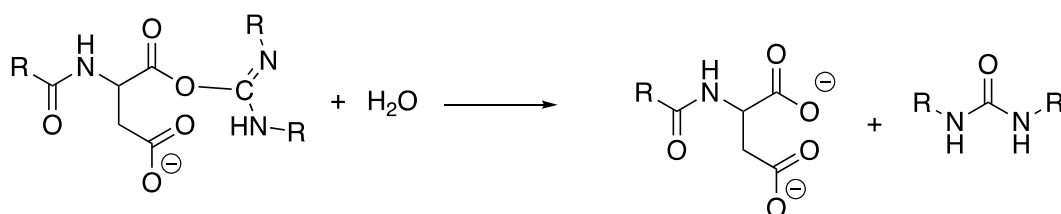
2) The formation of the anhydride with a first order rate constant. This rate constant could not be determined because the O-acylurea was never observed. It was therefore set to be twice the rate of  $k_1$ . As a result, the O-acylurea did never reach concentrations over 1  $\mu\text{M}$  in the model.

Reaction 2 ( $k_2$ )



3) Direct hydrolysis of O-acylurea ( $k_3$ ). This reaction rate could not be obtained because the O-acylurea was not observed. The ratio of  $k_2$  and  $k_3$  (anhydride formation and competing direct hydrolysis of O-acylurea) was varied to fit the HPLC data for several concentrations of  $[\text{fuel}]_0$  and  $[\text{di-acid}]_0$ .

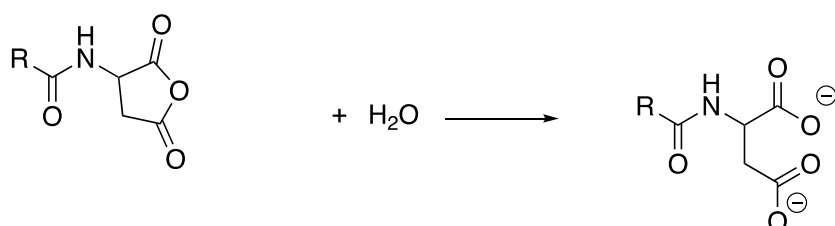
Reaction 3 ( $k_3$ )



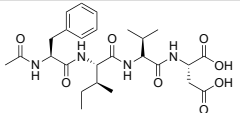
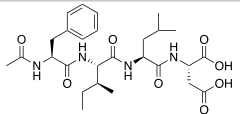
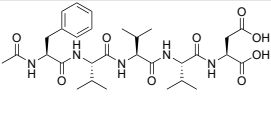
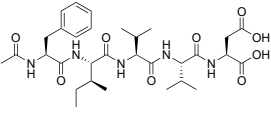
4) Hydrolysis of anhydride proceeded with a first order rate ( $k_4$ ) The rate constant was determined by HPLC for kinetic experiments where no assemblies were reached.

The rate of the hydrolysis reaction was calculated by multiplying the first order rate constant  $k_4$  with the concentration of anhydride.

Reaction 4 ( $k_4$ )



**Supporting Table S1. Characterization of precursors**

Name	Structure	Mass calculated [g/mol]	Mass observed [g/mol]	Retention time [min] @220nm	Purity
Ac-FIVD-OH <b>(P1)</b>		Mw = 534.27 $C_{26}H_{38}N_4O_8$	557.27 [Mw+Na] <sup>+</sup>	6.167	96%
Ac-FILD-OH <b>(P2)</b>		Mw = 548.28 $C_{27}H_{40}N_4O_8$	571.32 [Mw+Na] <sup>+</sup>	6.613	97%
Ac-FVVVD-OH <b>(P3)</b>		Mw = 619.32 $C_{30}H_{45}N_5O_9$	642.28 [Mw+Na] <sup>+</sup>	6.175	95%
Ac-FIVVD-OH <b>(P4)</b>		Mw = 633.34 $C_{31}H_{47}N_5O_9$	656.28 [Mw+Na] <sup>+</sup>	6.550	95%

**Supporting Table S2. Rate constants used to fit the HPLC data with a kinetic model.**

Name	$k_0$ (sec <sup>-1</sup> )	$k_1$ (M <sup>-1</sup> x sec <sup>-1</sup> )	$k_2$	$k_3$	$k_4$ (sec <sup>-1</sup> )
Ac-FIVD( <b>P1</b> )	$1.35 \times 10^{-5}$	$9 \times 10^{-2}$	$1.7 \cdot k_1$	$1 \cdot k_1$	$6 \cdot 10^{-3}$
Ac-FILD-OH ( <b>P2</b> )	$1.35 \times 10^{-5}$	$7.5 \times 10^{-2}$	$1.7 \cdot k_1$	$1 \cdot k_1$	$1 \cdot 10^{-2}$

## Supporting Figures

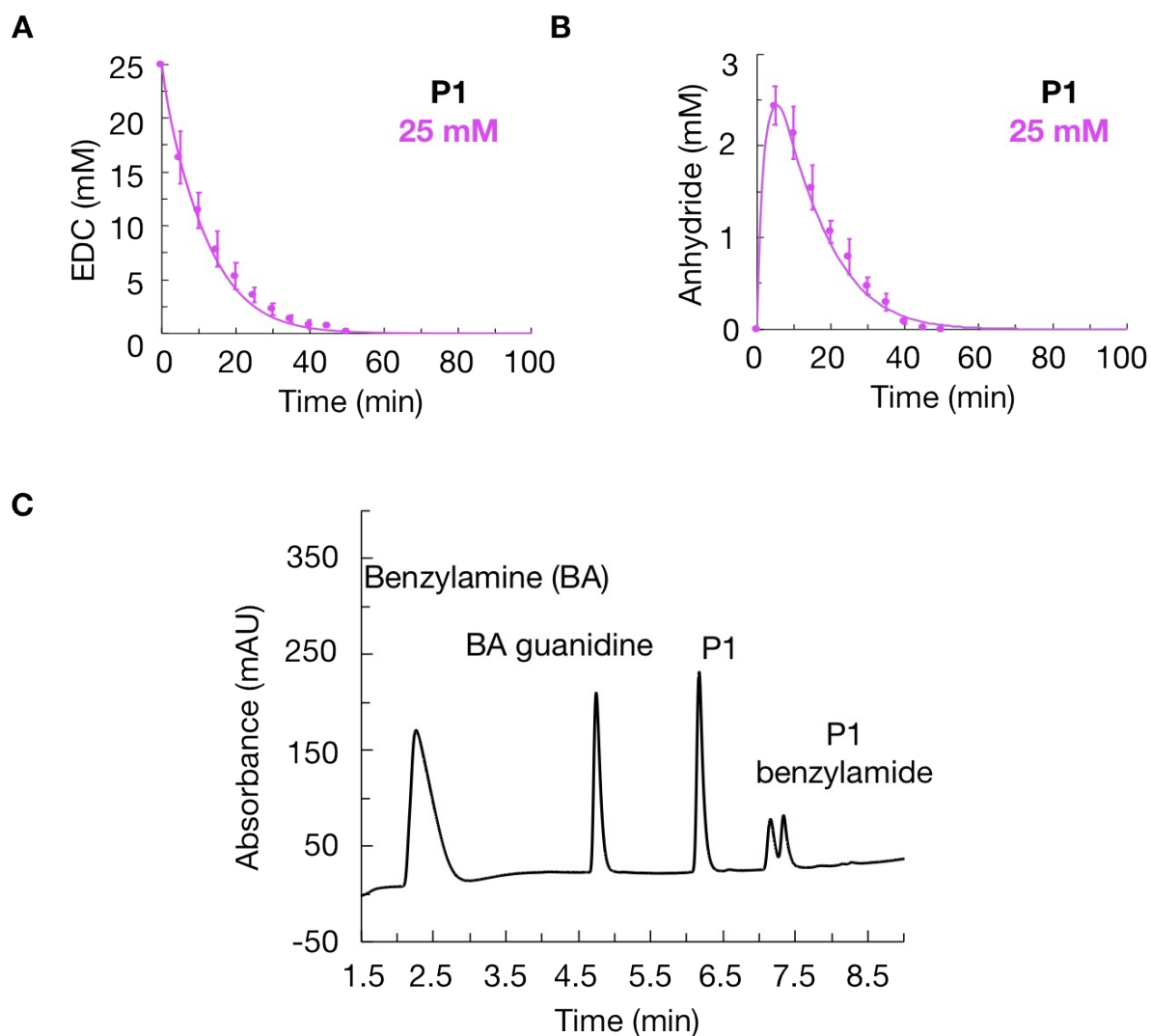


**Figure S1. Kinetic traces of P1 in the presence of fuel.** The concentration of EDC (A) and anhydride product (B) as a function of time when 10 mM P1 was fueled with 25 mM EDC. Error bars represent the standard deviation ( $n=3$ ). The lines represent data from the kinetic model, whereas the markers represent HPLC data. The kinetic traces can be fitted with a kinetic model that takes into account the hydrolysis occurring in solution<sup>2, 3</sup>. (C) Example of a chromatogram of 10 mM P1 with 25 mM EDC at 5 min after quenching with benzylamine (see Analytical HPLC Method).

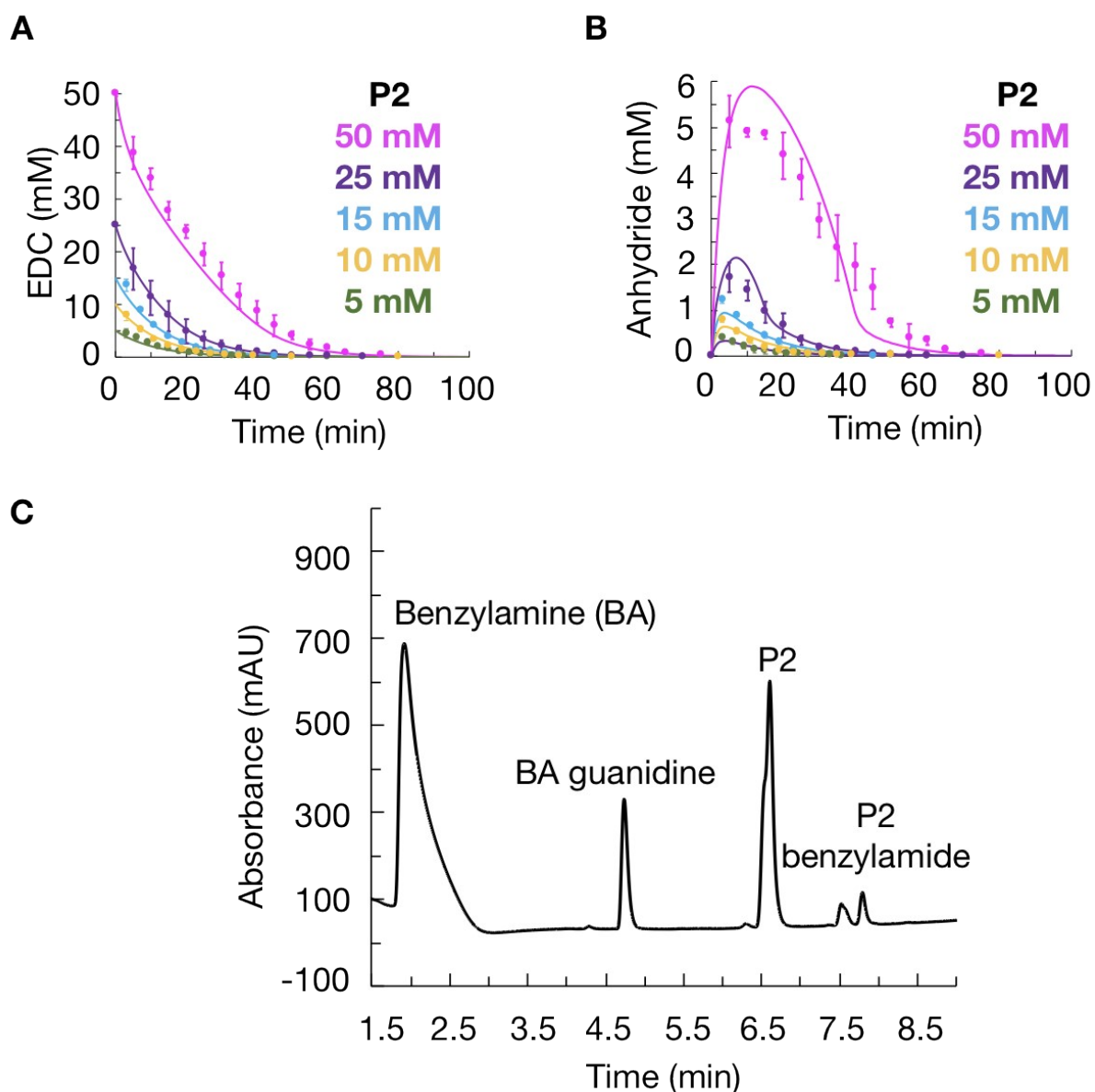


**Figure S2. Kinetic traces of P1 in the presence fuel.** The concentration of EDC (**A**) and anhydride product (**B**) as a function of time when 10 mM P1 was fueled with different concentrations of EDC. The kinetic traces can be fitted with a kinetic model that takes into account the hydrolysis occurring in solution<sup>2,3</sup>. The lines represent data from the kinetic model, whereas the markers represent HPLC data. Error bars represent the standard deviation ( $n=3$ ). (**C**) Example of a chromatogram of 10 mM P1 with 25 mM EDC at 10 min after quenching with benzylamine (see Analytical HPLC Method).

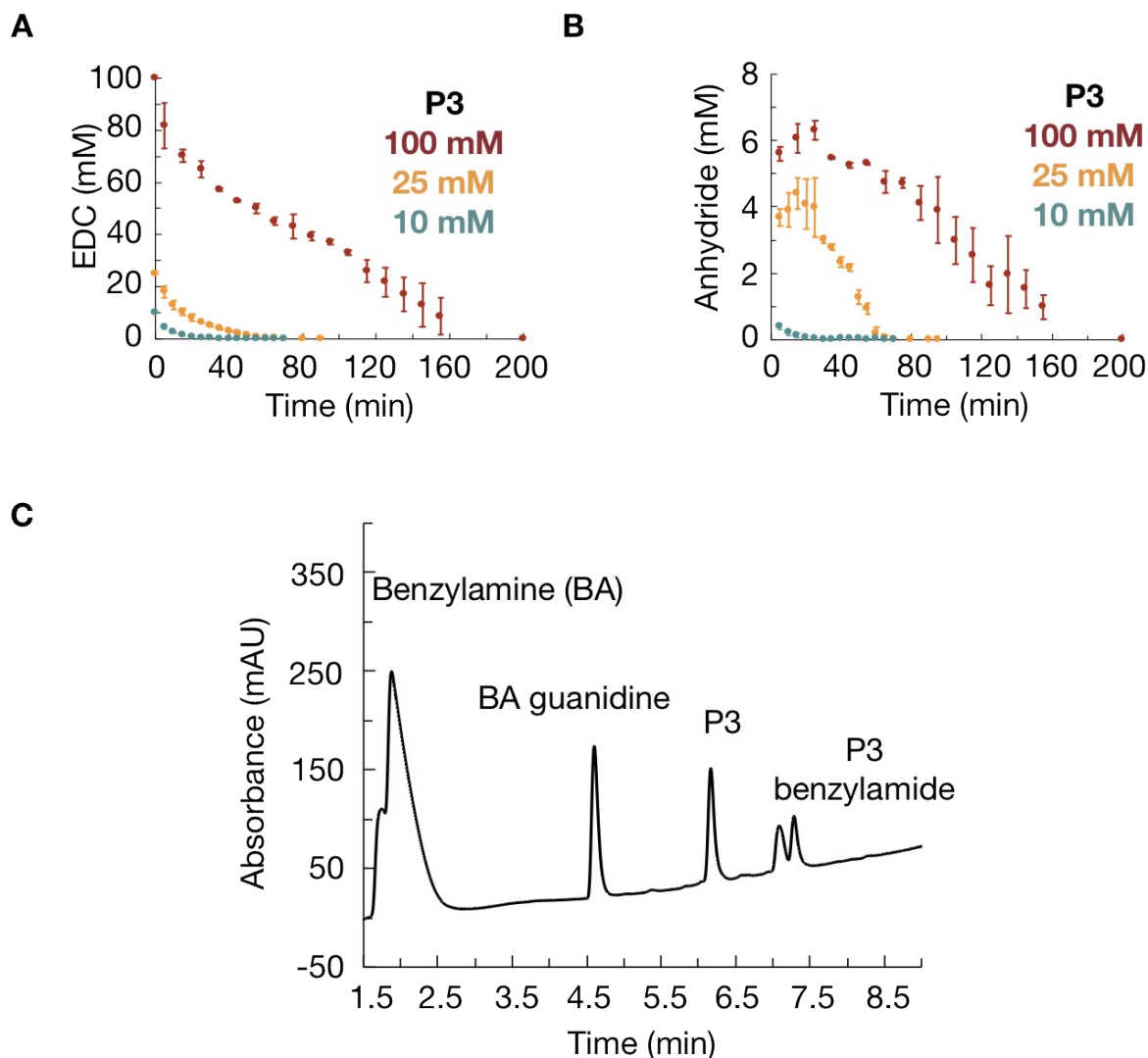


**Figure S3. Kinetic traces of P3 in the presence of fuel.** The concentration of EDC (A) and anhydride product (B) as a function of time when 10 mM P3 was fueled with different concentrations of EDC. Error bars represent the standard deviation ( $n=3$ ). (C) Example of a chromatogram of 10 mM P3 with 25 mM EDC at 5 min after quenching with benzylamine (see Analytical HPLC Method).

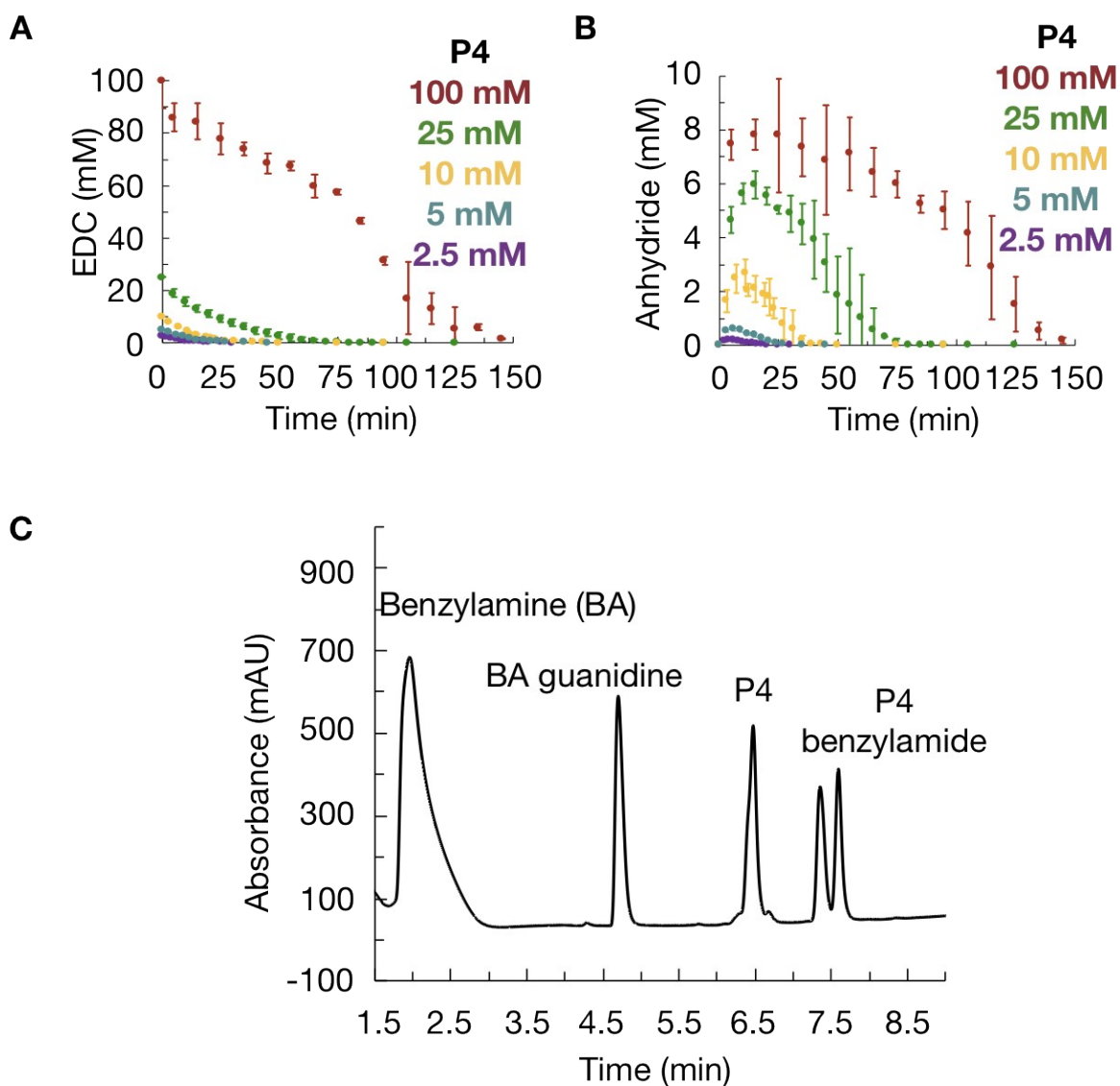


**Figure S4. Kinetic traces of P4 in the presence of fuel.** The concentration of EDC (**A**) and anhydride product (**B**) as a function of time when 10 mM P4 was fueled with different concentrations of EDC. Error bars represent the standard deviation ( $n=3$ ). (**C**) Example of a chromatogram of 10 mM P4 with 25 mM EDC at 5 min after quenching with benzylamine (see Analytical HPLC Method).

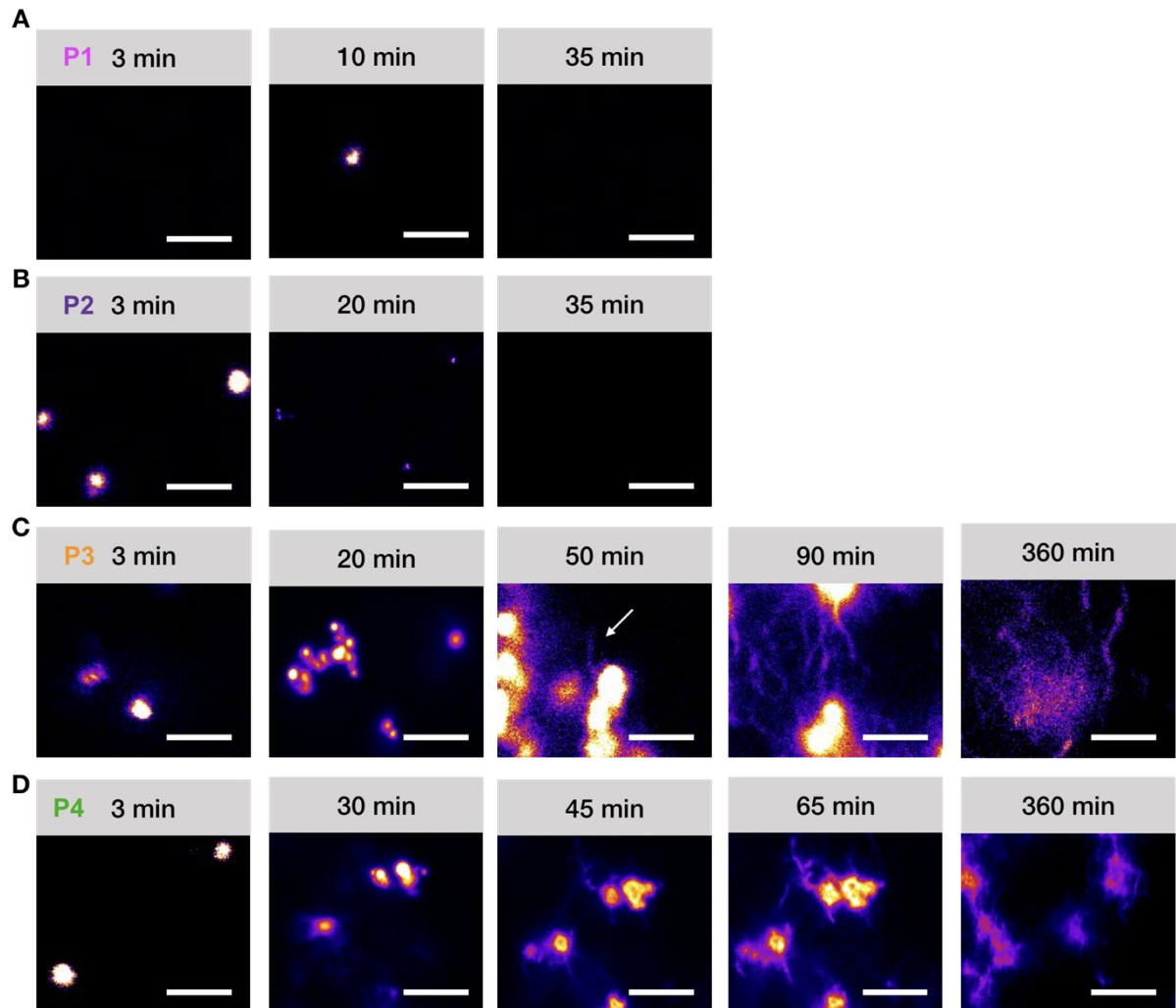


**Figure S5. Confocal micrographs.** *Confocal micrographs corresponding to the addition of 25 mM EDC to 10 mM P1 (A), 10 mM P2 (B), 10 mM P3 (C) and 10 mM P4 (D) over time. All scale bars correspond to 5  $\mu$ m. Samples were stained with 2.5  $\mu$ M Nile red.*

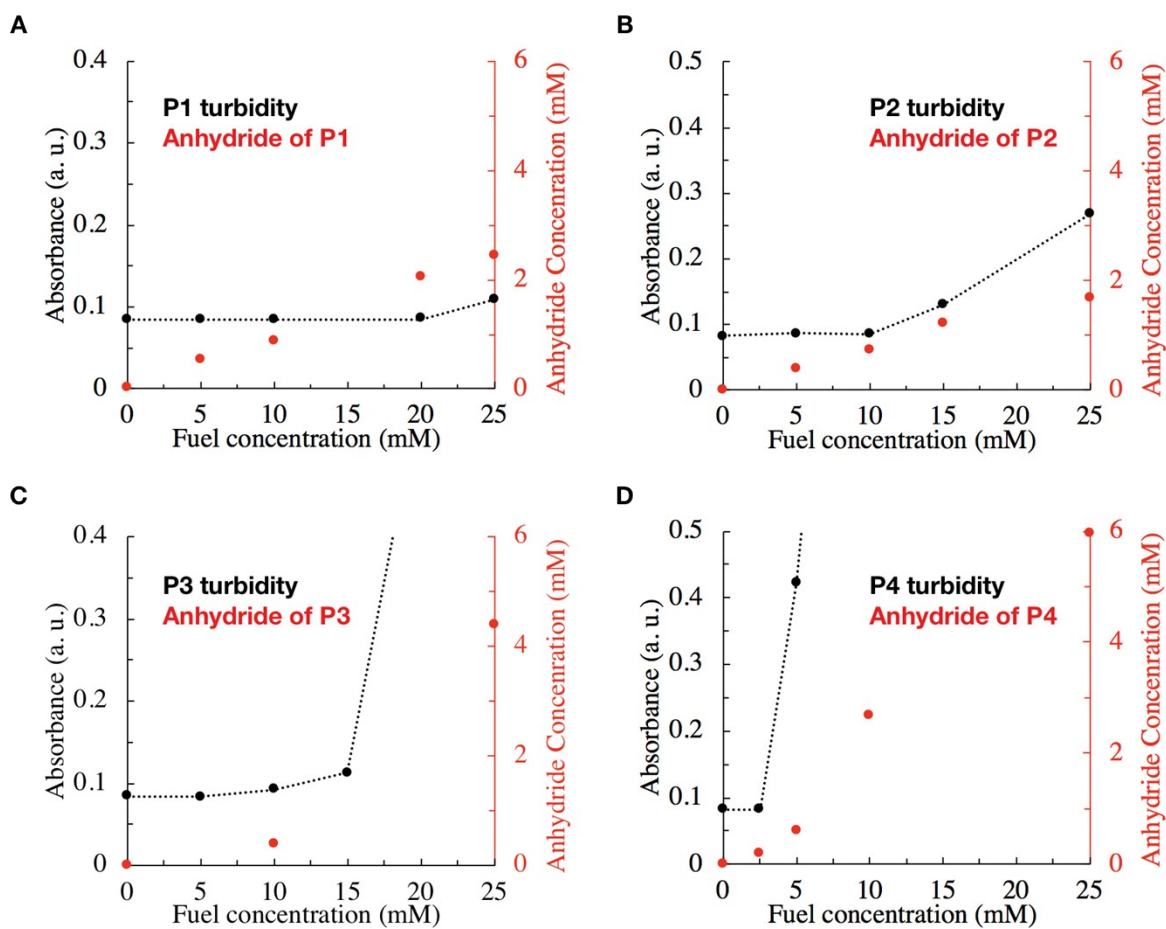


**Figure S6. Determination of the solubility of the anhydride.** (A) Anhydride concentration of **P1** and absorbance signal measured at 600 nm against fuel concentration. The solubility of the anhydride (2.2 mM) was averaged between the maximum anhydride concentration obtained with 25 mM fuel (first time turbidity was observed) and 20 mM of fuel (last time turbidity was not observed). (B) Anhydride concentration of **P2** and absorbance signal measured at 600 nm against fuel concentration. The solubility of the anhydride (1.1) was averaged between the maximum anhydride concentration obtained with 15 mM fuel (first time turbidity was observed) and 10 mM of fuel (last time turbidity was not observed). (C) Anhydride concentration of **P3** and absorbance signal measured at 600 nm against fuel concentration. The solubility of the anhydride (0.4 mM) was closed to the maximum anhydride concentration obtained with 10 mM fuel (first time turbidity was observed). (D) Anhydride concentration of **P4** and absorbance signal measured at 600 nm against fuel concentration. The solubility of the anhydride (0.2 mM) was averaged between the maximum anhydride concentration obtained with 5 mM fuel (first time turbidity was observed) and 2.5 mM of fuel (last time turbidity was not observed)

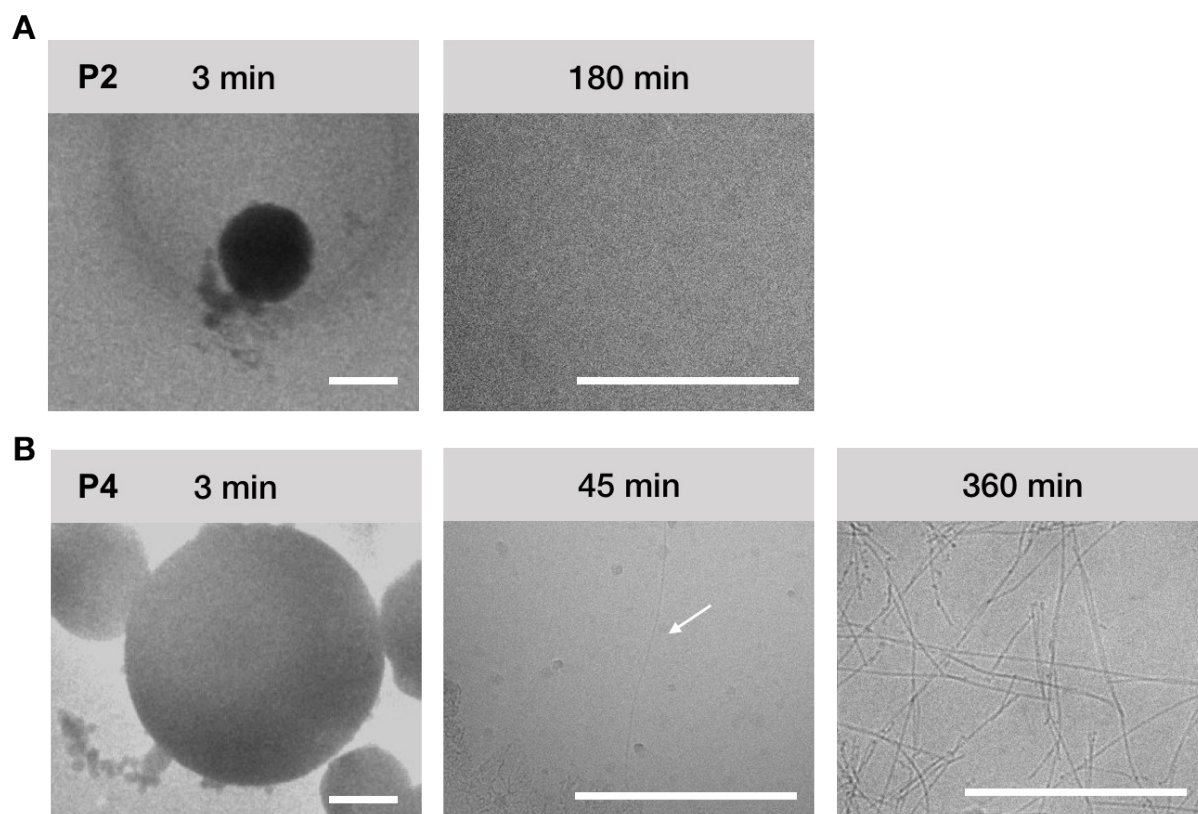


**Figure S7. Cryo-TEM micrographs.** All scale bars correspond to 100 nm. **Cryo-TEM micrographs** corresponding to the addition of 25 mM EDC to 10 mM **P2** (A) and 10 mM **P4** (B) over time. All scale bars correspond to 500 nm.

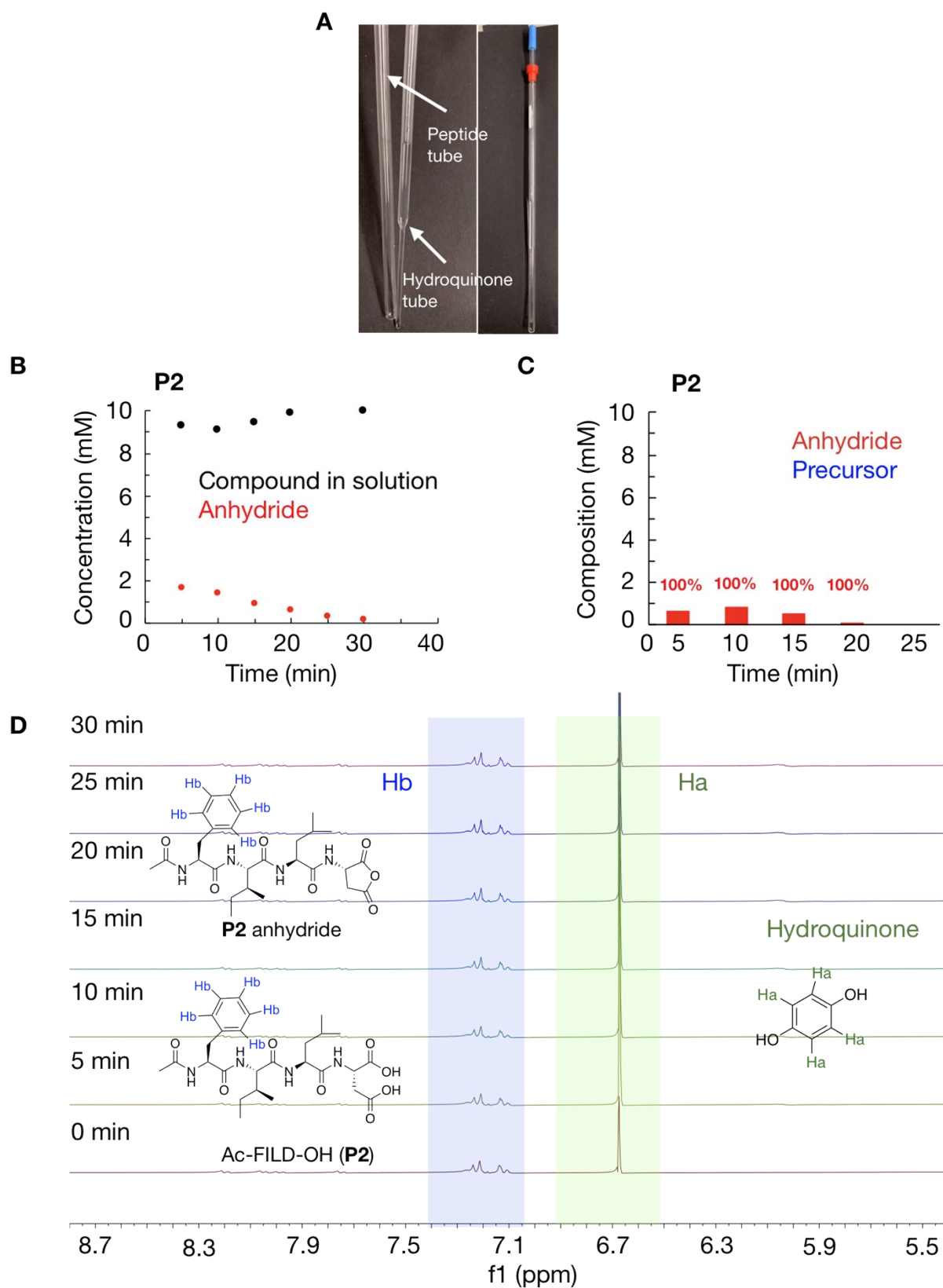


**Figure S8: The assembly composition of P2.** **A)** The scheme of NMR peptide tube and the inner tube with hydroquinone. **B)** The concentration of P2 precursor in solution as measured by NMR (black markers), and the concentration of P2 anhydride product as measured by



The concentration of **P3** precursor and **P3** anhydride in the assembly as a function of time that we calculated from the data in **A**:  $C_{in\ the\ assembly} = 10\ mM - C_{in\ the\ solution}$ . We assumed that, as long as there is still anhydride present in the solution, it is likely that there is no or only small amount of precursor in the assembled state. **C**)  $^1H$  NMR kinetics of **P3** (10 mM) after the addition of 25 mM of fuel. To determine the concentration of **P3** precursor and **P3** anhydride an internal standard (hydroquinone 50 mM in  $D_2O$ ) was used.

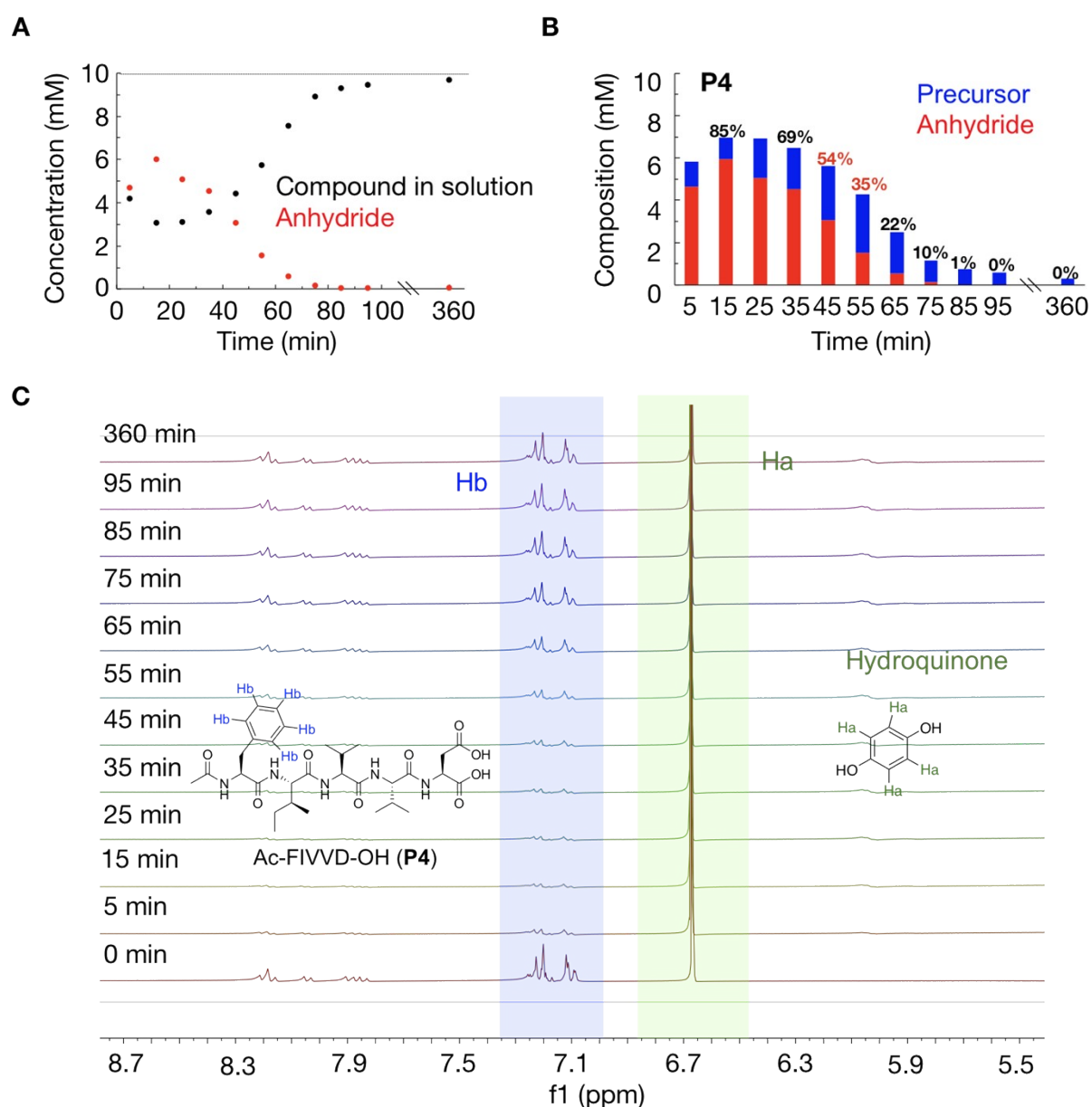


**Figure S10: The assembly composition of P4. A)** The concentration of **P4** precursor in solution as measured by NMR (black markers), and the concentration of **P4** anhydride product as measured by HPLC (red markers) as a function of time in response to 25 mM of EDC. **B)** The concentration of **P4** precursor and **P4** anhydride in the assembly as a function of time that we calculated from the data in **A**:  $C_{in\ the\ assembly} = 10\ mM - C_{in\ the\ solution}$ . **C)**  $^1H$  NMR kinetics of

**P4** (10 mM) after the addition of 25 mM of fuel. To determine the concentration of **P4** precursor and **P4** anhydride an internal standard (hydroquinone 50 mM in  $D_2O$ ) was used.

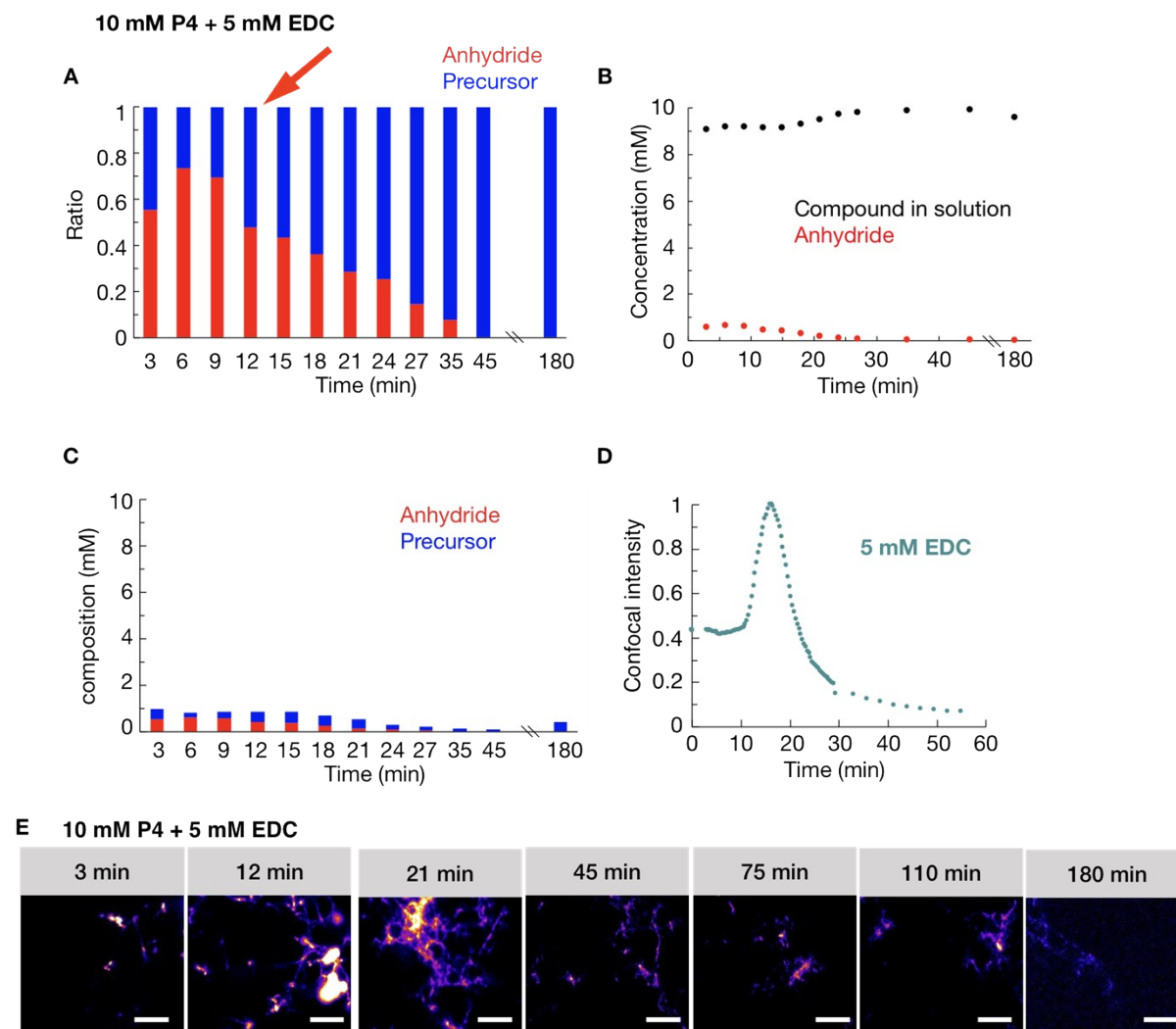


**Figure S11: The assembly composition and the confocal microscopy for P4 with 5 mM Fuel.** **A)** The ratio of anhydride and precursor in the assembly over time determined by HPLC and NMR for 10 mM **P4** after the addition of 5 mM of fuel. **B)** The concentration of **P4** precursor in solution measured by NMR (black markers), and the concentration of **P4** anhydride product measured by HPLC as a function of time (red markers) in response to 5 mM of EDC. **C)** The concentration of **P4** precursor and **P4** anhydride in the assembly as a function of time that we calculate from the data in **A**:  $C_{in\ the\ assembly} = 10\ mM - C_{in\ the\ solution}$ . We assumed that, as long as there is still anhydride present in the solution, it is likely that there is no or only small amount of precursor in the assembled state. **D)** The normalized intensity from confocal microscopy for 10 mM **P4** with 5 mM EDC as a function of time. **E)** Confocal micrographs of **P4** (10 mM) after the addition of 5 mM EDC over time. All scale bars correspond to 5  $\mu m$ . Samples were stained with 2.5  $\mu M$  Nile red. The red arrow indicates the point where around 55% of anhydride is in the assembly.

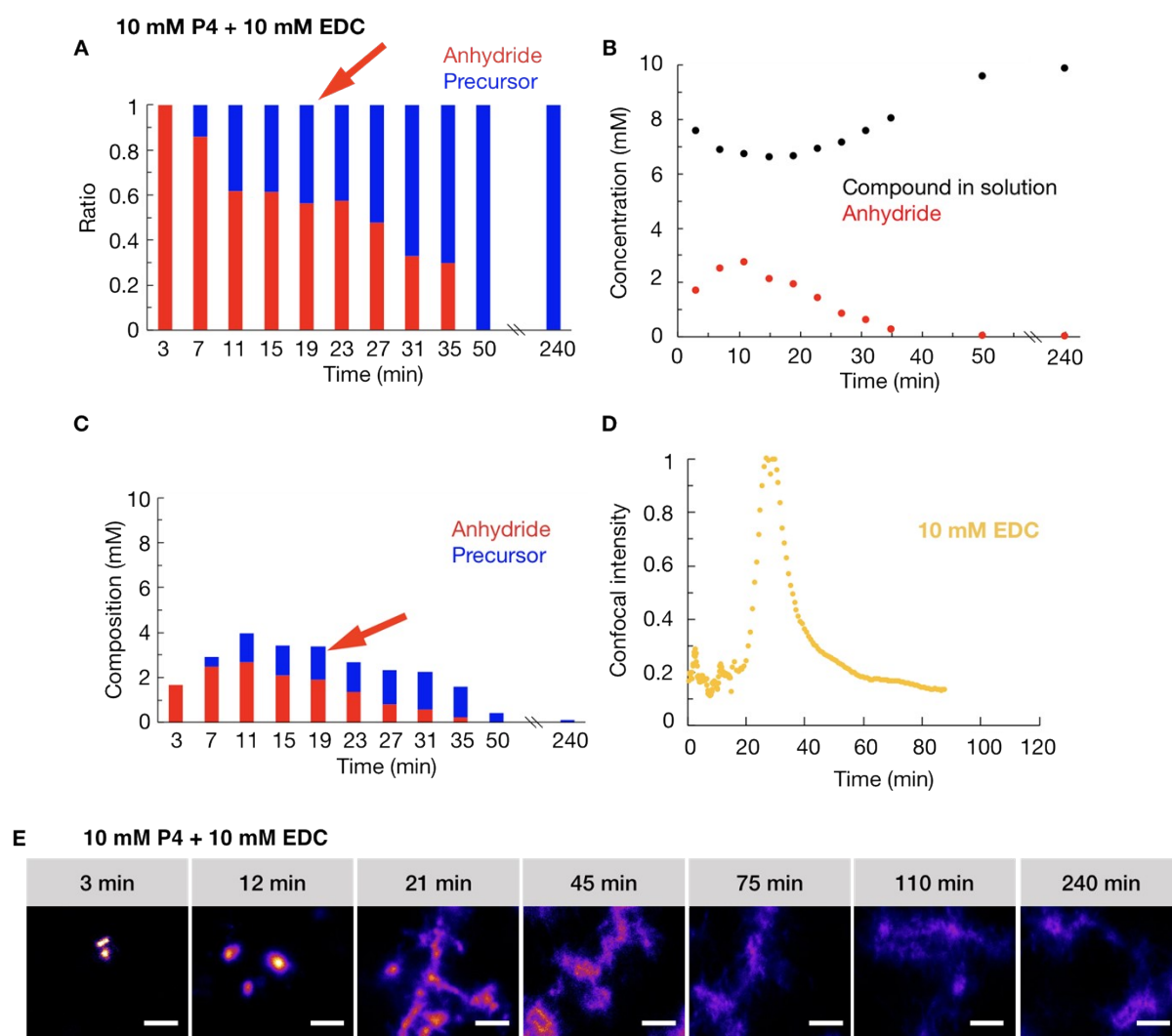


**Figure S12: The assembly composition and the confocal microscopy for P4 with 10 mM Fuel.** **A)** The ratio of anhydride and precursor in the assembly over time determined by HPLC and NMR for 10 mM P4 after the addition of 10 mM of fuel. **B)** The concentration of P4 precursor in solution measured by NMR (black markers), and the concentration of P4 anhydride product measured by HPLC as a function of time (red markers) in response to 10 mM of EDC. **C)** The concentration of P4 precursor and P4 anhydride in the assembly as a function of time that we calculate from the data in **A**:  $C_{in\ the\ assembly} = 10\ mM - C_{in\ the\ solution}$ . **D)** The normalized intensity from confocal microscopy for 10 mM P4 with 10 mM EDC as a function of time. **E)** Confocal micrographs of P4 (10 mM) after the addition of 10 mM EDC over time. All scale bars correspond to 5  $\mu$ m. Samples were stained with 2.5  $\mu$ M Nile red. The red arrow indicates the point where around 55% of anhydride is in the assembly.

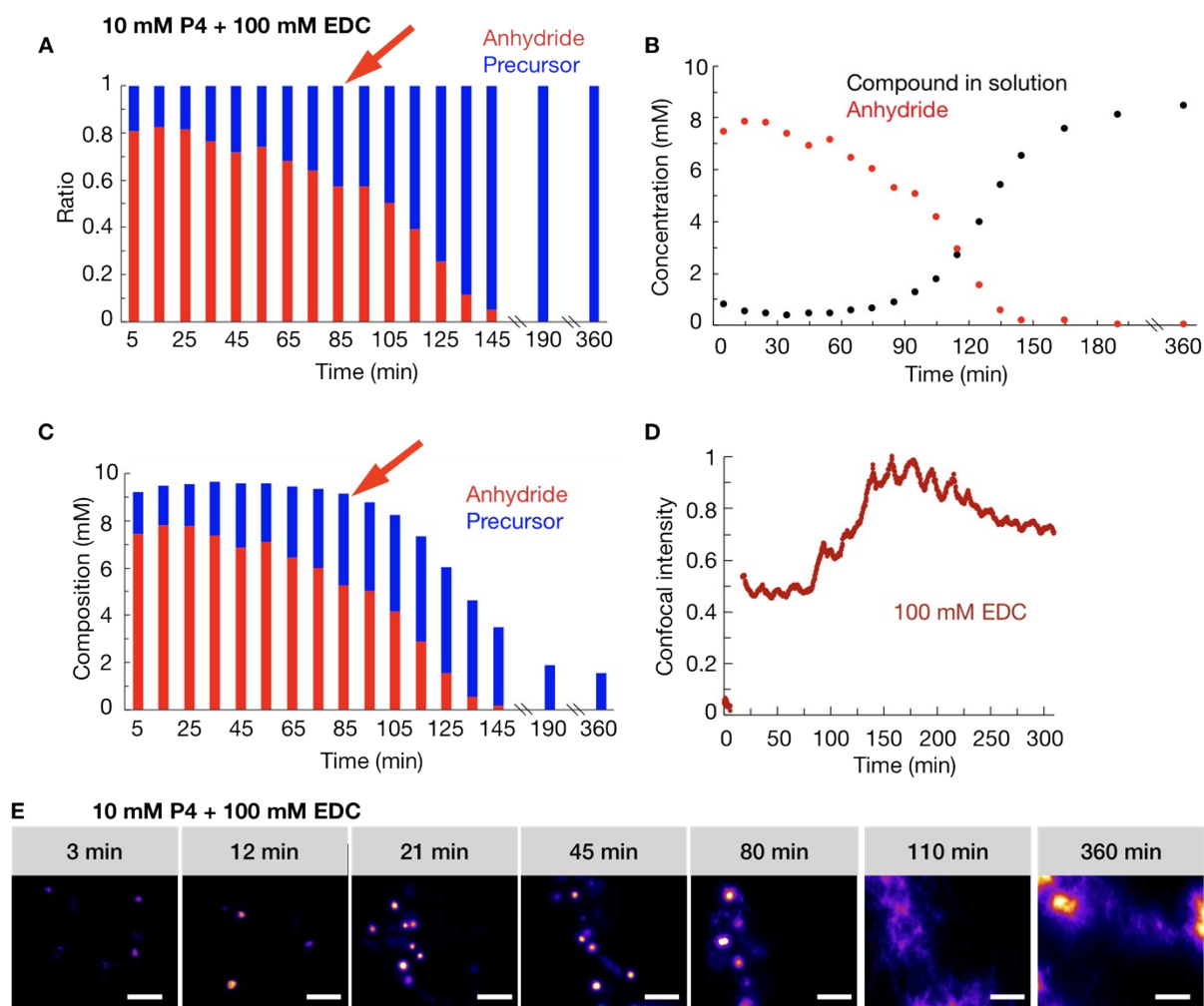


**Figure S13: The assembly composition and the confocal microscopy for P4 with 100 mM Fuel.** **A)** The ratio of anhydride and precursor in the assembly over time determined by HPLC and NMR for 10 mM P4 after the addition of 100 mM of fuel. **B)** The concentration of P4 precursor in solution measured by NMR (black markers), and the concentration of P4 anhydride product measured by HPLC as a function of time (red markers) in response to 100 mM of EDC. **C)** The concentration of P4 precursor and P4 anhydride in the assembly as a function of time that we calculate from the data in **A**:  $C_{in\ the\ assembly} = 10\ mM - C_{in\ the\ solution}$ . **D)** The normalized intensity from confocal microscopy for 10 mM P4 with 100 mM EDC as a function of time. **E)** Confocal micrographs of P4 (10 mM) after the addition of 100 mM EDC over time. All scale bars correspond to 5  $\mu$ m. Samples were stained with 2.5  $\mu$ M Nile red. The red arrow indicates the point where around 55% of anhydride is in the assembly.

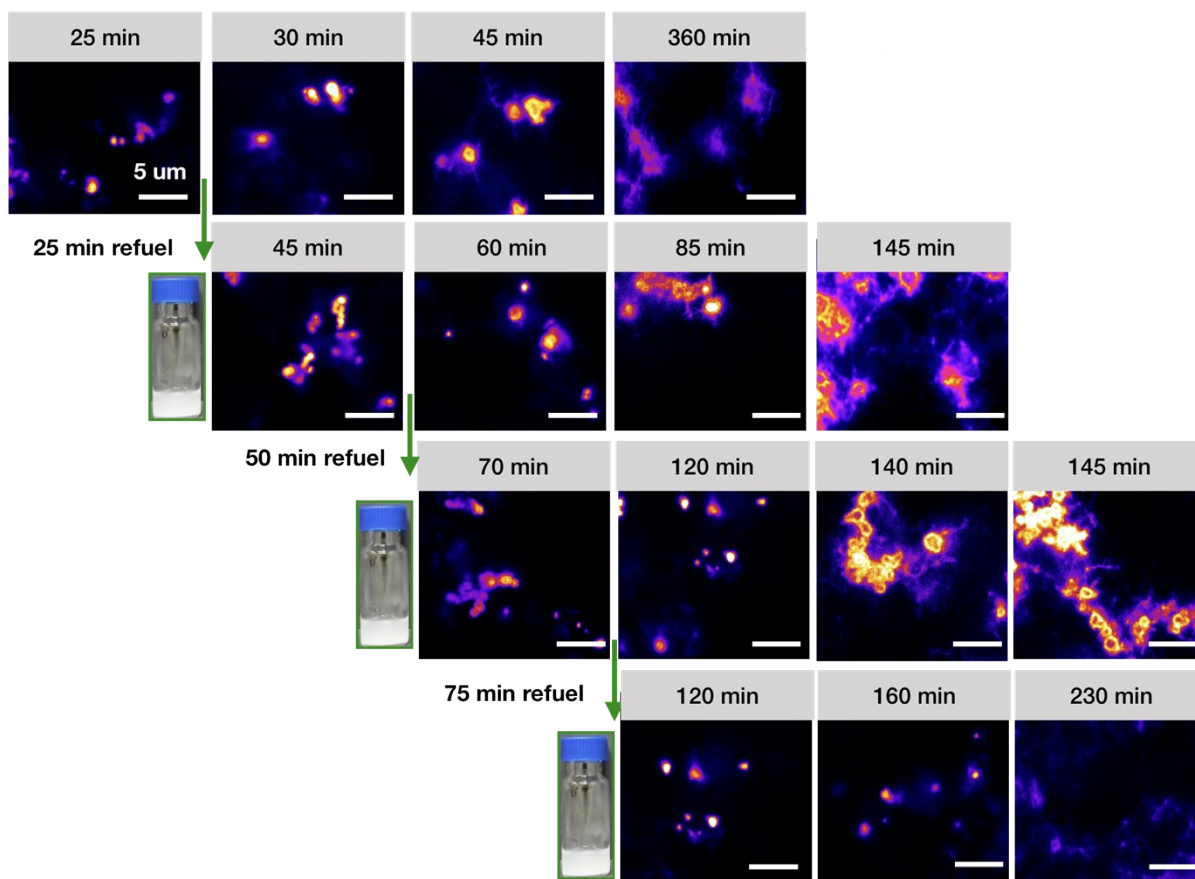


**Figure S14: Confocal micrograph of P4 (10 mM) with EDC refueling (25 mM) every 25 minutes. All scale bars correspond to 5 μm. The dye for confocal is 2.5 μM Nile red.**

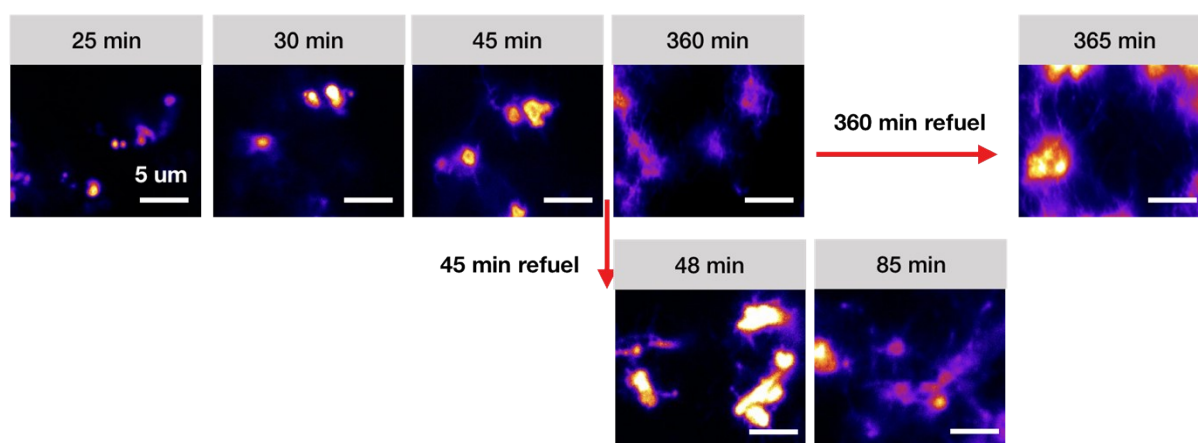


**Figure S15: Confocal micrograph of 25 mM EDC refuel to 10 mM P4 with 25 mM EDC system after fiber formation. All scale bars correspond to 5 μm. Samples were stained with 2.5 μM Nile red.**

1. F. Schnitter and J. Boekhoven, *ChemSystemsChem*, 2020, **3**.
2. B. Riess, C. Wanzke, M. Tena-Solsona, R. K. Grotsch, C. Maity and J. Boekhoven, *Soft Matter*, 2018, **14**, 4852-4859.
3. M. Tena-Solsona, B. Riess, R. K. Grotsch, F. C. Lohrer, C. Wanzke, B. Kasdorf, A. R. Bausch, P. Muller-Buschbaum, O. Lieleg and J. Boekhoven, *Nat Commun*, 2017, **8**, 15895.